A THEORETICAL INVESTIGATION OF 2-2 COMPOSITE TRANSDUCERS WITH HIGH SHEAR ATTENUATION IN THE PASSIVE PHASE

L-A. Orr[†], A. J. Mulholland[†,*], R.L. O'Leary[‡] and G. Hayward[‡]

[†] Department of Mathematics, University of Strathclyde, Glasgow, UK

‡ Department of Electrical and Electronic Engineering, University of Strathclyde, Glasgow, UK

[*] ajm@maths.strath.ac.uk

Composite piezoelectric transducers have many advantages but the periodic pillar architecture also gives rise to unwanted lateral modes which interfere with the piston like motion of the main thickness mode. In this paper we use a three dimensional plane wave expansion model (PWE) of these transducers, which incorporates viscoelastic losses, to examine the dispersive behaviour of a 2-2 composite transducer with high shear attenuation in the passive phase. The identification of the modes is aided by examining profiles of the displacements, electrical potential and Poynting vector. The model shows that the use of a high shear attenuation filler material improves the transmission bandwidth of the device by damping out unwanted lateral modes.

1 Introduction

Piezoelectric composite transducers are increasingly becoming the design of choice in biomedical, sonar and nondestructive testing applications [1]. The most frequently used designs are made by dicing the ceramic into a series of pillars and then filling the void with a passive polymer phase (see Figure 1) . For a 2-2 composite the ceramic is cut longitudinally in one direction so that there is connectivity in two directions for both the ceramic and polymer. However, one of the problems with this architecture is the presence of surface waves, which are generated between the adjacent pillars (inter-pillar modes) or within the pillars (intra-pillar modes), interfering with the piston like behaviour of the main thickness mode. Extensive experimental observations have highlighted the intricate dependency between the geometry of the design, the material properties and the key operational characteristics of the device. It has been suggested that a passive material with a low transverse coupling would enhance the transducer's efficiency [2], [3].

We have recently extended the 3-dimensional plane wave expansion model (PWE) derived by Wilm et al [4] to incorporate frequency dependent, viscoelastic losses [5]. We will use this model to examine the dispersive behaviour of a 2-2 composite transducer and investigate the effects of introducing high shear attenuation into the passive phase. The aim is to increase the frequency band gap between the thickness mode and other parasitic waves to obtain a higher transmission bandwidth. The identification of the modes is aided by examining profiles of the displacements, electrical potential and Poynting vector. As mentioned above finite element modelling (FEM)[1] can lose important information on low amplitude modes and high frequency modes but since the PWE method operates in the frequency domain no such restrictions apply.

Section 2 by provides a brief outline of the plane wave expansion method following the derivation of Wilm et al [4] . In Section 3 a composite transducer with a high shear loss passive phase is analysed. Plots of the electrical conductance and a modal analysis using displacement and Poynting vector profiles are used to discuss the operating characteristics of this device.

2 Formulation of the method

2.1 The geometry

The model is configured for periodic 1-3 composites with thickness in the x_3 direction. We use the periodicity of the structure to expand the material constants, $M(r)$ say, as Fourier series where M represents either the density ρ, the elasticity tensor c_{ijkl}, the piezoelectric stress tensor e_{ijk}, or the permittivity tensor ϵ_{ij}.

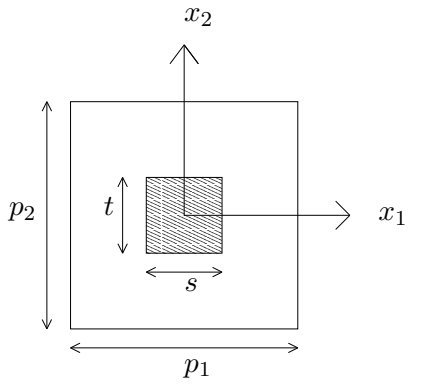

(a)

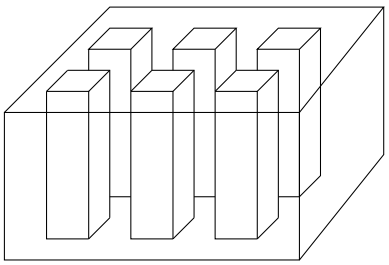

(b)

Figure 1: (a) Plan view of the x_1-x_2 plane and (b) three-dimensional geometry over a few periods of the model.

For the composite structure shown in Figure 1 the material constants only depend on x_1 and x_2. We denote by p_1 the periodicity in the x_1 direction and by p_2 the periodicity in the x_2 direction. The width of the ceramic pillar in the x_1 and x_2 direction is denoted by s and t, respectively. For the 2-2 composites considered here we need simply set $t = p_2$. The dependent variables $F(r,t)$ propagating within these periodic structures are then approximated as a Floquet series

$$F(r,t,k,\omega) = \sum_{s=1}^{(2N+1)^2} F^s(k,\omega) e^{\jmath(\omega t - k\cdot r - G^s\cdot r)} \tag{1}$$

where $r = (x_1, x_2, x_3)$, t is time, ω is the angular frequency, $k = (k_1, k_2, k_3)$ is the wave vector, $G^s = \left(\frac{2\pi}{p_1}H^{s,1}, \frac{2\pi}{p_2}H^{s,2}, 0\right)$ and H is an ordered set of Fourier coefficient indices.

2.2 The Model

The piezoelectric constitutive equations together with Newton's second law and Gauss's law for dielectric media are [6]

$$T_{ij} = c_{ijkl}u_{k,l} + e_{lij}\phi_{,l} \tag{2}$$

$$D_i = e_{ikl}u_{k,l} - \epsilon_{il}\phi_{,l} \tag{3}$$

$$\rho\frac{\partial^2 u_j}{\partial t^2} = T_{ij,i} \tag{4}$$

$$D_{i,i} = 0. \tag{5}$$

Equations (2) to (5) constitute 16 equations in the 16 unknowns which are the stresses T_{ij}, the displacements u_k, the electric potential ϕ and the electrical displacements D_i . The notation can be compacted by defining a generalized displacement field u where $u = (u_1, u_2, u_3, u_4 = \phi)$ and three generalized stress vectors $t_i = (T_{i1}, T_{i2}, T_{i3}, D_i)$. Substituting the Fourier description of the material properties and expansion (1) into these four equations we obtain, after some manipulations (see [4] for full details), the generalised eigenvalue problem

$$\begin{bmatrix} \omega^2 R - B & 0 \\ -C_2 & I \end{bmatrix} \begin{pmatrix} U \\ \jmath T_3 \end{pmatrix} = k_3 \begin{bmatrix} C_1 & I \\ D & 0 \end{bmatrix} \begin{pmatrix} U \\ \jmath T_3 \end{pmatrix} \tag{6}$$

in the $8(2N+1)^2$ eigenvalues $k_3^{(r)}$ and corresponding eigenvectors $\begin{bmatrix} U \\ \jmath T_3 \end{bmatrix}^{(r)}$ where R, B, C_i and D are large matrices containing the material Fourier coefficients and wavenumbers k_1 and k_2. Solving equation (6) and introducing the relative amplitudes $A^{(r)}$ we get

$$\begin{pmatrix} u(r,t) \\ t_3^q(r,t) \end{pmatrix} = e^{\jmath(\omega t - k_1 x_1 - k_2 x_2)} \times \sum_{q=1}^{(2N+1)^2} e^{-\jmath G^q\cdot r} \left(\sum_{r=1}^{8(2N+1)^2} A^{(r)} e^{-\jmath k_3^{(r)} x_3} \begin{bmatrix} u^q \\ t_3^q \end{bmatrix}^{(r)} \right). \tag{7}$$

Energy distribution within the transducer can be used to clarify particular types of modes in conjunction with examining the profiles of the displacements, stresses and electric potential. To examine the energy we use the Poynting vector defined as

$$P_j = -T_{ij}u_{i,t} + \phi D_{j,t}. \tag{8}$$

Substituting equations (2) and (3) into equation (8) and since $u_{k,t} = \jmath\omega u_k$ by equation (1), then

$$P_j = -\jmath\omega(c_{ijkl}u_{k,l}+e_{lij}\phi_{,l})u_i+$$

$$\jmath\omega\phi(e_{jkl}u_{k,l} - \epsilon_{jl}\phi_{,l}). \tag{9}$$

2.3 Boundary Conditions

The method is sufficiently general to cope with a wide range of boundary conditions but for simplicity we shall consider the mechanical boundary conditions of a stress free plate. From equation (7) we have,

$$0 = \sum_{r=1}^{8(2N+1)^2} A^{(r)}e^{-\jmath k_3^{(r)}h}[T_{3i}^q]^{(r)}, \tag{10}$$

and

$$0 = \sum_{r=1}^{8(2N+1)^2} A^{(r)}[T_{3i}^q]^{(r)}. \tag{11}$$

For the electrical boundary conditions we fix the electrical potential at the top and bottom of the transducer. The surface potential is defined as

$$\phi(x_1, x_2, t) = V_0 e^{\jmath(\omega t-\gamma_1 x_1-\gamma_2 x_2)}, \tag{12}$$

where $\gamma_i = k_i p_i/(2\pi)$ (i=1,2) denotes the electrode spacing, nondimensionalised as the ratio of the pillar width to the wavelength. From equation (7) we can then show that at $x_3 = h$

$$\sum_{r=1}^{8(2N+1)^2} A^{(r)}\phi^{q,(r)}e^{-\jmath k_3^{(r)}h} = V_0\{\mathrm{sinc}\{(k_1+$$

$$G_1^q)\frac{p_1}{2}\}\} \times \{\mathrm{sinc}\{(k_2 + G_2^q)\frac{p_2}{2}\}\} \tag{13}$$

and at $x_3 = 0$

$$\sum_{r=1}^{8(2N+1)^2} A^{(r)}\phi^{q,(r)} = 0. \tag{14}$$

Equations (10), (11), (13) and (14) constitute $8(2N+1)^2$ equations in the $8(2N+1)^2$ unknowns $A^{(r)}$. Hence we can solve this system of linear equations and examine the displacements, stresses etc. using equation (7).

One advantage of studying piezoelectric composites is that the electrical operating characteristics provide an alternative means of deriving the dispersion curves. The admittance (Y) expresses the ease with which the alternating current flows through the transducer and the resonant modes are signified by a maxima in the real part of the admittance. Using continuity of the electrical potential at the front interface we obtain [4]

$$Y(k_1, k_2, \omega) = \jmath\omega \sum_{q=1}^{(2N+1)^2}\{\sum_{r=1}^{8(2N+1)^2} A^{(r)}\times$$

$$\left(D_3^{q,(r)} - \epsilon_0|\kappa|\phi^{q,(r)}\right)e^{-\jmath k_3^{(r)}h}\}(p_1\,\mathrm{sinc}((k_1+$$

$$G_1^q)\frac{p_1}{2}))(p_2\,\mathrm{sinc}((k_2+G_2^q)\frac{p_2}{2})) \tag{15}$$

where $\kappa = \sqrt{(k_1 + G_1^q)^2 + (k_2 + G_2^q)^2}$.

3 Results

The methodology presented in the previous section is illustrated here by investigating the modal behaviour of a 2-2 composite transducer composed of 70% PZT5H ceramic and 30% HY1300/CY1301 polymer (see Tables 1 and 2 for details). The saw pitch (p_1) is 2mm, the kerf width (s) is 1.4mm and the thickness (h) is 2mm. In the polymer phase the shear wave attenuation coefficient is 356db/m whilst the longitudinal wave attenuation coefficient is 139db/m, both measured at 0.5MHz. In the ceramic phase the viscoelastic loss tangent is 1/65.

By examining the conductance as a function of the electrode spacing γ_1 in Figure 2, the thickness mode can be identified as the central

Physical Property	Value
G'(kg m^{-1}s^{-2})	1.57×10^9
Y'(kg m^{-1}s^{-2})	4.28×10^9
ρ (kg m^{-3})	1.149×10^3
ϵ	4
c_{11}	7.1977×10^9
c_{44}	1.5739×10^9

Table 1: Physical properties of the polymer phase

Constant	Units	Value
C_{11}	Nm^{-2}	12.72×10^{10}
C_{12}	Nm^{-2}	8.02×10^{10}
C_{13}	Nm^{-2}	8.47×10^{10}
C_{33}	Nm^{-2}	11.74×10^{10}
ϵ_{33}	-	1700
ϵ_{11}	-	1470
ρ_b	kg m^{-3}	7.5×10^3
e_{33}	C m^{-2}	23.3
e_{31}	C m^{-2}	-6.5

Table 2: Physical properties of the ceramic phase

ridge of the plot at around 0.65MHz. The lower frequency maxima correspond to Lamb waves whilst the inter/intra-pillar modes are the first set of peaks to the right of the thickness mode at around 1MHz. The advantages of plotting the conductance is that we can clearly see the relative importance of each mode and in this way it eradicates any spurious modes found in the

dispersion diagram. The electrical conductance of the transducer can be used to examine the effect of varying the loss in the passive phase (see Figure 3).

A modal analysis shows that the thickness mode is at $f = 0.6478$MHz and the first antisymmetric Lamb wave (a_0 mode) is at $f = 0.117$MHz. When high shear loss is introduced it is apparent that there is a damping effect on all modes except the thickness mode. Figure 4 shows the high shear loss gradually taking effect in a plot of the absolute value of the electrical impedance of the transducer as a function of the driving frequency and the degree of shear attenuation in the passive phase. The aim is to damp out any unwanted modes around the electrical resonant frequency, which corresponds to the thickness mode.

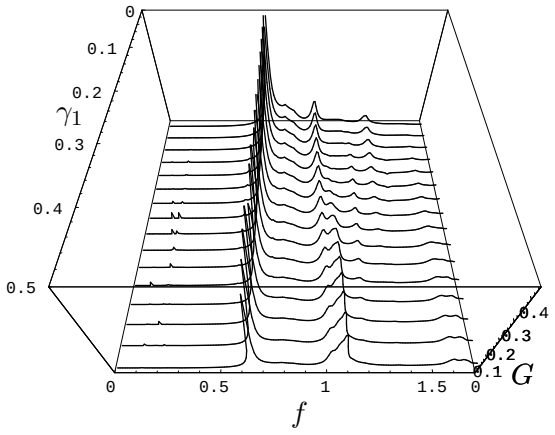

Figure 2: The conductance of the transducer G (normalised) plotted against the electrode spacing γ_1 and the driving frequency f (MHz) for a 2-2 composite transducer with low shear attenuation.

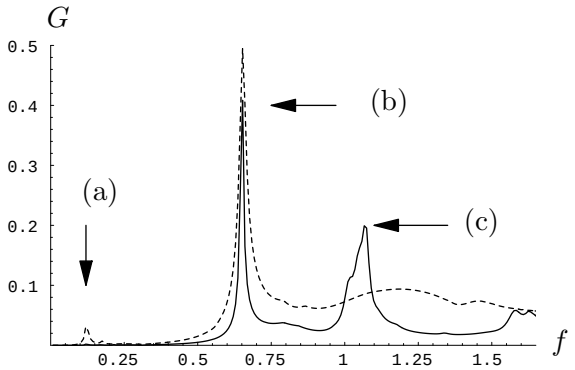

Figure 3: Conductance (G) versus frequency (fMHz) for a 2-2 composite transducer. The solid and dash line represent low shear attenuation (a) $a_0$mode, (b) thickness mode and (c) interpillar mode and high shear attenuation respectively.

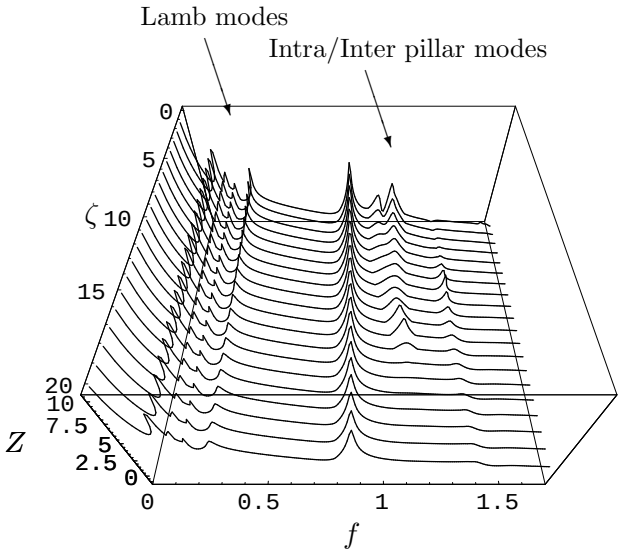

Figure 4: The absolute value of the electrical impedance of the transducer Z (normalised) versus frequency (f) and passive phase shear loss scaling (ζ) for a 2-2 composite transducer.

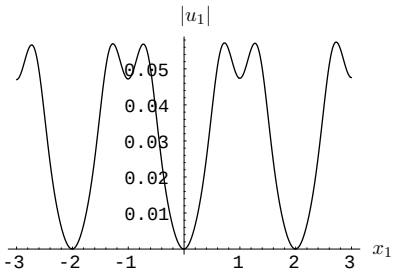

(a)

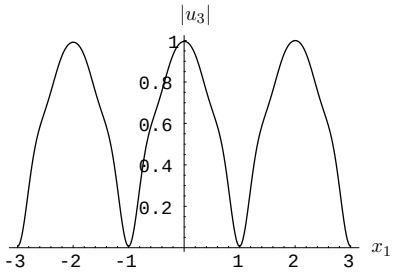

(b)

Figure 5: Normalised displacement of a 2-2 composite transducer at the thickness mode for low shear attenuation in the passive phase during excitation. Plot (a) shows the in-plane displacement and plot (b) shows the out of plane component of displacement as x_1 is varied (at $x_3 = 0$) ($f = 0.6478$ MHz, $k_1 = 1.5 + 0.001\jmath$ mm^{-1}).

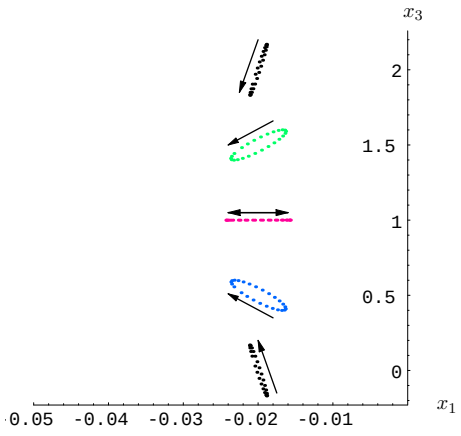

(a)

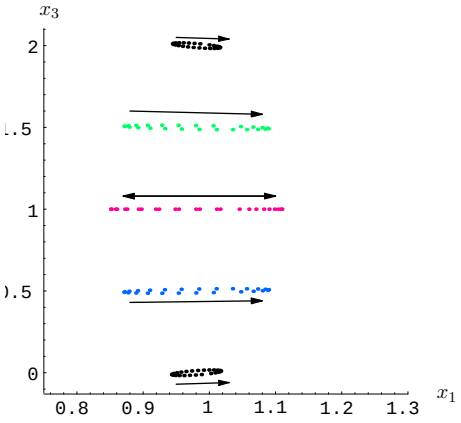

(b)

Figure 6: Displacement of a 2-2 composite transducer at the thickness mode for low shear attenuation in the passive phase during excitation. Plot (a) illustrates the movement of specific points within the ceramic phase as time is varied and (b) illustrates the movement of specific points over time within the polymer phase ($f = 0.6478$ MHz, $k_1 = 1.5 + 0.001\jmath$ mm^{-1}).

From the impedance curve Figure 3 we see that as the degree of attenuation (ζ) is increased both the Lamb modes and intra/interpillar modes are being damped.

3.1 Modal Analysis

The standard classification of the modes is problematic here as the supporting medium is heterogeneous, anisotropic, lossy and piezoelec-

tric. As such the descriptions of the waves in terms of their symmetry, or as Lamb, Rayleigh, bulk waves etc. are only psuedo-descriptions and the actual behaviour is far more complex. Identification of modes is aided by spatial and/or temporal plots of the displacement, the Poynting vector and the electrical potential. In Figure 5, for example, the lateral displacement (u_1) is negligible compared to the displacement in the thickness direction (u_3), which has its largest values at the faces of the transducer, within the ceramic. Of course this is at one instant in time and it is useful to examine the temporal evolution of various spatially fixed reference points within the device. Figure 6 shows that the ceramic pillars are moving vertically with very little motion in the lateral direction (x_1) (note the axes scales), however the polymer is being pulled sideways with no motion in the thickness (x_3) direction. The in-plane Poynting vector can be viewed by proportionally displacing its components to show where the energy is stored. For example, Figure 7 shows that the energy is distributed throughout the transducer, primarily in the thickness direction. The symmetrical displacement profile in both directions, the large amplitude of oscillation and the dominant displacement being in the thickness direction all point to this being the thickness mode.

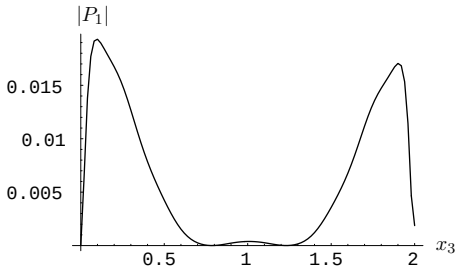

(a)

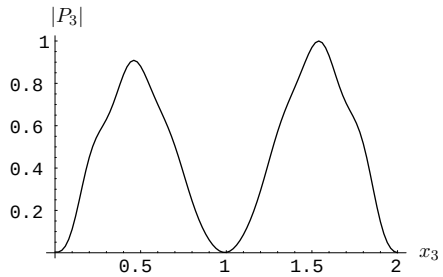

(b)

Figure 7: Normalised Poynting vector of a 2-2 composite transducer at the thickness mode for low shear attenuation in the passive phase. Plots (a) and (b) show the components of the Poynting vector as x_3 is varied (at $x_1 = 0$) ($f = 0.6478$ MHz, $k_1 = 1.5 + 0.001\jmath$ mm^{-1}).

4 Conclusions

The plane wave expansion (PWE) method is a frequency domain approach for analysing the modal behaviour of periodic, anisotropic, piezoelectric composites. We have extended the method to include frequency dependent viscoelastic losses in both the ceramic and polymer phases. One advantage of this approach over time domain methods is that information on low amplitude or high frequency modes is not lost. Conductance spectra for low and high shear attenuation in the passive phase were compared and this showed that the use of a high shear loss polymer damps unwanted lateral modes and results in an improved bandwidth around the thickness mode. One advantage of piezoelectric composites is that the electrical characteristics provide an additional means of examining the mechanical wave dispersion properties.

This approach can circumvent the numerical instabilities and lengthy computation times associated with the standard modal analysis which relies on the identification of the zeros of the determinant of a large, ill-conditioned matrix. Although the standard classification of the modes is problematic, as the supporting medium is heterogeneous, anisotropic, lossy and piezoelectric, we are able to give pseudo-descriptions of the main supported modes of vibrations using spatial and/or temporal plots of the displacement, the Poynting vector and the electrical potential. We are currently investigating the extension of the model to more irregular geometries, and conducting a quantitative comparison with finite element predictions and experimental measurements. Our longer term goal is to develop the method to include realistic operating conditions such as backing and matching layers, electrical and mechanical loads and finite lateral dimensions.

References

[1] G. Hayward and J. Hyslop, "Lamb Wave Generation in Periodic Piezoelectric Composite Array Substrates, Part 1: Theory and Experimental Measurements", IEEE UFFC, 53(2), pp. 443-448, 2006.

[2] T.R. Gururaja, W.A. Schulze, L.E. Cross, R.E. Newnham, B.A. Auld and Y.J. Wang, "Piezoelectric composite materials for ultrasonic transducer applications. Part 1: Resonant modes of vibration of PZT rod-polymer composites", IEEE Trans Sonics and Ultrasonics, SU-22(4), pp. 481-498, 1985.

[3] T.R. Gururaja, W.A. Schulze, L.E. Cross and R.E. Newnham, "Piezoelectric composite materials for ultrasonic transducer applications. Part 2: Evaluation of ultrasonic medical applications", IEEE Trans Sonics and Ultrasonics, SU-22(4), pp. 499-513, 1985.

[4] M. Wilm, S. Ballandras, V. Laude and T. Pastureaud, "A Full 3D Plane-Wave-Expansion Model for 1-3 Piezoelectric Composite Structures", JASA, 112(3), pp. 943-952, 2002.

[5] L-A. Orr, A.J. Mulholland, R. O'Leary and G. Hayward, "Incorporation of Frequency Dependent, Viscoelastic Loss in a Plane Wave Expansion Model of 1-3 Composite Transducers", (submitted to JASA).

[6] "IEEE Standard on Piezoelectricity", IEEE Trans UFFC, 43(5), pp717, 1996.